

Vector-borne diseases with non-stationary vector populations: the case of growing and decaying populations

Àlex Giménez-Romero^a, Rosa Flaquer-Galmés^{a,b}, Manuel A. Matias^{a,*}

^a*IFISC (CSIC-UIB), Instituto de Física Interdisciplinar y Sistemas Complejos, Campus UIB
E-07122 Palma de Mallorca, Spain*

^b*Grup de Física Estadística, Departament de Física. Facultat de Ciències, Universitat Autònoma de Barcelona,
08193 Bellaterra (Barcelona), Spain*

Abstract

Since the last century, deterministic compartmental models have emerged as powerful tools to predict and control epidemic outbreaks, in many cases helping to mitigate their impacts. A key quantity for these models is the so-called *Basic Reproduction Number*, R_0 , that measures the number of secondary infections produced by an initial infected individual in a fully susceptible population. Some methods have been developed to allow the direct computation of this quantity provided that some conditions are fulfilled, such that the model has a pre-pandemic disease-free equilibrium state. This condition is only fulfilled when the populations are *stationary*. In the case of vector-borne diseases, this implies that the vector birth and death rates need to be balanced, what is not fulfilled in many realistic cases in which the vector population grow or decrease. Here we develop a vector-borne epidemic model with growing and decaying vector populations and study the conditions under which the standard methods to compute R_0 work and discuss an alternative when they fail. We also show that growing vector populations produce a delay in the epidemic dynamics when compared to the case of the stationary vector population. Finally, we discuss the conditions under which the model can be reduced to the SIR model with fewer compartments and parameters, which helps in solving the problem of parameter unidentifiability of many vector-borne epidemic models.

Keywords: Epidemics, Vector-borne diseases, Basic Reproduction Number, Compartmental model, Mathematical model

1. Introduction

Vector-borne diseases are caused by infectious agents transmitted by living organisms, called vectors, frequently arthropods. These diseases represent a significant threat to global human health (Athni et al., 2020), causing diseases such as malaria, dengue, yellow fever, Zika, trypanosomiasis and leishmaniasis (Schumacher & Campbell, 2018). Vector-borne human diseases are responsible of more than 17% of all human infectious diseases, causing millions of cases and more than 700 000 deaths annually (WHO). Moreover, crop production and farm profitability are also affected by bacterial (Huang et al., 2020) and virus (Bragard et al., 2013) vector-borne diseases. Some examples are the Pierce’s Disease of grapevines, that has resulted in an annual cost of approximately \$100 million in California alone (Tumber et al., 2014), the olive quick decline syndrome, which could cause about \$5 and 17 billion of loss in Italy and Spain over the next 50 years in the absence of disease control measures (Schneider et al., 2020) and the multiple diseases caused by viruses (Rybicki, 2015), with diseases like the tobacco mosaic, tomato spotted wilt, etc. and transmitted by aphids and other vectors.

Compartmental deterministic models, e.g. the well known SIR model (Kermack & McKendrick, 1927), have been widely used in the modelling of vector-borne diseases after the work of Ross and Macdonald (Macdonald, 1957), that, opened the way to controlling malaria outbreaks by acting on

*Corresponding author

Email address: manuel@ifisc.uib-csic.es (Manuel A. Matias)

the vectors of the disease (the *Anopheles* mosquito). These models consider that both host and vector populations can be divided into different compartments describing different states of the individuals, such as susceptible, infected or dead (Brauer, 2008), and the time-evolution of these compartments is expressed as a system of ordinary differential equations, defining a dynamical system. Compartmental models provide a mean-field description, that imply well-mixed (in practice spatially homogeneous) populations. The well mixed approximation will be valid whenever the mean distance among hosts is smaller than the mixing length of vectors before they die. In the case of vector-borne diseases it is also equivalent to every vector effectively interacting with all the hosts and every host with all the vectors. A mean-field description is not always valid in spatially extended systems, but still it is normally the first step before writing a spatially explicit description.

The most relevant piece of information about a disease is whether an epidemic outbreak will take place. The *basic reproduction number*, R_0 , measures the number of secondary infections caused by an initial infected individual in a fully susceptible population, defining the epidemic threshold (Anderson, 1991; van den Driessche, 2017), that determines the emergence (or not) of an outbreak. If $R_0 > 1$ an epidemic outbreak will occur, while there will be no outbreak otherwise. The standard way of determining R_0 in deterministic compartmental models assumes the existence of an initial disease-free (pre-pandemic) equilibrium, represented by the absence of infected hosts and vectors (Laukó, 2006; Kamgang & Sallet, 2008). Some standard methods based on the linear stability condition of this equilibrium have been developed to allow the direct computation of R_0 , such as the Next-Generation Matrix (NGM) method (Diekmann et al., 2010).

In the case of vector-borne diseases models typically assume that populations (both hosts and vectors) do not change with time (see e.g. (Macdonald, 1957; Brauer et al., 2016)), assuming equal birth and death rates. This guarantees the existence of a disease-free equilibrium and the proper use of standard methods to determine R_0 . However, this assumption could be far from reality in several pathosystems. In particular, the interaction between temperature, precipitation variations and other factors may lead to strong variations in the vector population (Garms et al., 1979; Rocklöv & Dubrow, 2020), implying that the pre-pandemic state may not be an equilibrium state and that standard methods cannot be applied.

Some authors have explicitly considered more general cases in which the demographic rates are not identical or even time-dependent with a given periodicity. In the case of unbalanced birth and death rates one obtains an asymptotic stationary vector population, but not an initial disease-free equilibrium, except in the case that the initial vector population coincides with the asymptotic value. Nevertheless, the basic reproduction number of these models is often computed by means of the standard methods from the asymptotic state of the population (Wei et al., 2008; Lashari & Zaman, 2011; Shah & Jyoti, 2013; Zhao et al., 2020; Esteva & Vargas, 1998). The use of these methods is supported by the fact that the asymptotic dynamics of the system under study can be described by the subsystem in which the vector population is in its stationary value (Thieme, 1992; Castillo-Chavez & Thieme, 1995). Indeed in (Esteva & Vargas, 1998) it is explicitly pointed out that “it is enough to study the asymptotic behaviour of the model”. In the case of periodic demographic rates it has been shown that the time-averaged basic reproduction number defines the epidemic threshold under some circumstances (Wesley & Allen, 2009) and even a generalisation of the NGM method (Diekmann & Heesterbeek, 2000) has been developed for these cases (Bacaër & Guernaoui, 2006; Bacaër, 2007).

Compartmental models of vector-borne diseases have another feature that may hinder their practical applicability. Namely the fact that these models have many compartments, having to describe both hosts and vectors, and as a consequence a relatively large number of parameters. This may lead to an issue known as *parameter identifiability and uncertainty* (Chowell, 2017), depending on the available data, that is more likely to be found in models with many compartments and parameters (Roosa & Chowell, 2019). Usually, parameter estimation procedures are needed to connect the models with disease data, mainly using incidence or prevalence over time in the host population. Unfortunately, under many circumstances the underlying model parameters are unidentifiable, so that many different sets of parameter values produce the same model fit (Kao & Eisenberg, 2018). Moreover, these parameters can be really difficult to determine from the available experimental data. Nevertheless, in some cases, mathematical manipulations can be performed to reduce the model complexity using exact or approximate relations (Giménez-Romero et al., 2021). In such cases, the number of parameters of the models can be usually reduced in terms of new

parameters defined as combinations of some of the original parameters.

The plan of this paper is as follows. In [Section 2](#) we develop a compartmental model of vector-borne transmitted diseases with constant, but different, birth and death rates for the vectors, which allow us to describe growing and decaying vector populations. For simplicity, the model assumes that there is no horizontal (host to host) direct transmission, which is also a realistic assumption in some cases, like plant diseases. [Section 3](#) contains the main results of the study. In particular, we show how and when traditional methods fail to estimate the R_0 of the model and provide an alternative way to compute it. It turns out that the validity of the standard methods depends, among other things, on some time-scales of the model. Furthermore, we discuss and apply some approximations that allow to reduce the model in favour of simpler ones, with both fewer compartments and fewer parameters. In particular, we show that if some of the parameters fulfil certain conditions, it is possible to reduce the original model with five compartments and four parameters to a SIR model, with three compartments and two parameters. It is expected that model reductions like this one significantly help in solving possible problems of parameter unidentifiability that plague these models. It is interesting to note that a model in which hosts do not interact directly, but only through vectors, in a certain limit becomes described as if hosts would infect one to each other, what is assumed in some studies without suitable confirmation. Finally, the main concluding remarks of the study are presented in [Section 4](#).

2. The model

The compartment model for vector-borne diseases that we will use to illustrate the points to be discussed in this study consists of 5 compartments, 3 of which describe the host population (susceptible, S_H , infected, I_H , and removed, R_H), while the other 2 describe the vector population (susceptible S_V and infected vectors, I_V). Thus, we consider that the pathogen affects only the hosts and do not consider exposed compartments. In addition, no horizontal (direct host to host) or vertical (mother to offspring for vectors) transmission is assumed. The model could be also generalised to include an exposed host compartment and the above mentioned transmission modes, which would hinder the theoretical analysis without altering the qualitative conclusions of the study. Anyhow, the absence of horizontal transmission would make the model adequate to study vector-borne diseases in which host-to-host infection is rare, like malaria, and most phytopathologies, although not for, say, zika. Finally, we do not consider host recruitment neither infected hosts becoming susceptible again.

The model is defined according to the following processes,

$$S_H + I_V \xrightarrow{\beta} I_H + I_V \quad I_H \xrightarrow{\gamma} R_H \quad S_V + I_H \xrightarrow{\alpha} I_V + I_H \quad S_V \xrightarrow{\mu} \emptyset \quad I_V \xrightarrow{\mu} \emptyset, \quad (1)$$

which are graphically described in [Fig. 1](#), being the birth of new susceptible vectors described as a source term. Thus, the host-vector compartmental model is written as,

$$\begin{aligned} \dot{S}_H &= -\beta S_H I_V / N_H \\ \dot{I}_H &= \beta S_H I_V / N_H - \gamma I_H \\ \dot{R}_H &= \gamma I_H \\ \dot{S}_V &= \delta C - \alpha S_V I_H / N_H - \mu S_V \\ \dot{I}_V &= \alpha S_V I_H / N_H - \mu I_V, \end{aligned} \quad (2)$$

where a standard incidence ([Martcheva, 2015](#)) has been considered.

The model describes infection of susceptible hosts, S_H , at a rate β through their interaction with infected vectors, I_V , while susceptible vectors, S_V , are infected at a rate α through their interaction with infected hosts I_H . Infected hosts exit the infected compartment at rate γ , while infected vectors stay infected the rest of their lifetime, as we consider that the pathogen does not affect them, as it is customary. Vectors die naturally (or disappear from the population by some mechanism) at rate μ and are born (appear) at a constant rate δ being susceptible. The constant term C sets the scale of the stationary value of the vector population. [Fig. 1](#) shows an schematic representation of the model and we refer to ([Brauer et al., 2016](#)) for a similar model of vector-borne

diseases. The mentioned model includes exposed compartments and horizontal transmission, but assumes that the birth and death rate of vectors are identical, and thus, the population does not change with time and stays as fixed by the initial condition.

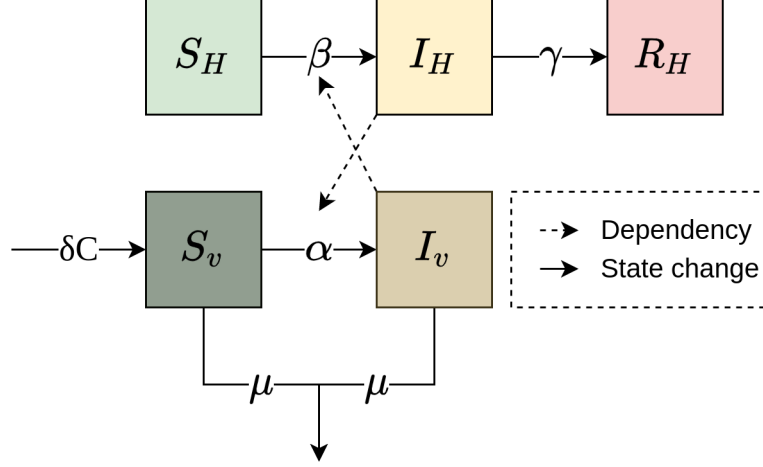


Figure 1: Schematic representation of the model in Eq. (2). Boxes are the compartments in which the population is divided, solid arrows represent changes in state (so transitions between compartments), and dashed arrows depict the crossed interaction between hosts and vectors.

2.1. Preliminary analysis of the model

From Eq. (2) it is straightforward to verify that the population of hosts remains constant over time, $N_H = S_H + I_H + R_H$, while the vector population fulfils,

$$\dot{N}_v = \dot{S}_v + \dot{I}_v = -\mu(S_v + I_v) + \delta C = -\mu N_v + \delta C, \quad (3)$$

which can be solved to yield,

$$N_v(t) = \frac{\delta}{\mu} C + \left(N_v(0) - \frac{\delta}{\mu} C \right) e^{-\mu t}. \quad (4)$$

From Eq. (4) the stationary value for the vector population, N_v^* , can be computed as,

$$N_v^* = \lim_{t \rightarrow \infty} N_v(t) = \frac{\delta}{\mu} C. \quad (5)$$

Thus, if the initial population of vectors is below (above) the stationary value, the vector population will grow (decrease) until it reaches the stationary value. On the other hand, if $N_v(0) = N_v^* = \delta C / \mu$ the initial population of vectors is already at the stationary state. The initial condition for the vector population can be written in terms of its stationary value Eq. (5), $N_v(0) = f N_v^*$, where both $f < 1$ and $f > 1$ are possible, so that one gets,

$$N_v(t) = N_v^* [1 + (f - 1) e^{-\mu t}]. \quad (6)$$

We note that vector-borne disease models that assume constant vector populations (e.g. (Brauer et al., 2016)) can be recovered by setting $\delta = \mu$ and $C = N_v(0)$, so that any initial condition for the vector population is stationary, i.e. $\dot{N}_v = 0$ in Eq. (3) and $N_v(t) = N_v(0)$.

3. Results

3.1. The effect of non-stationary vector populations into the epidemic threshold and disease dynamics

Let us start with the case in which the birth δ and death μ vector rates are identical and the initial condition of the vector population is already at its stationary value, $N_v(0) = N_v^*$, case in which the total vector population remains unchanged, as discussed in Section 2.1. In such a case,

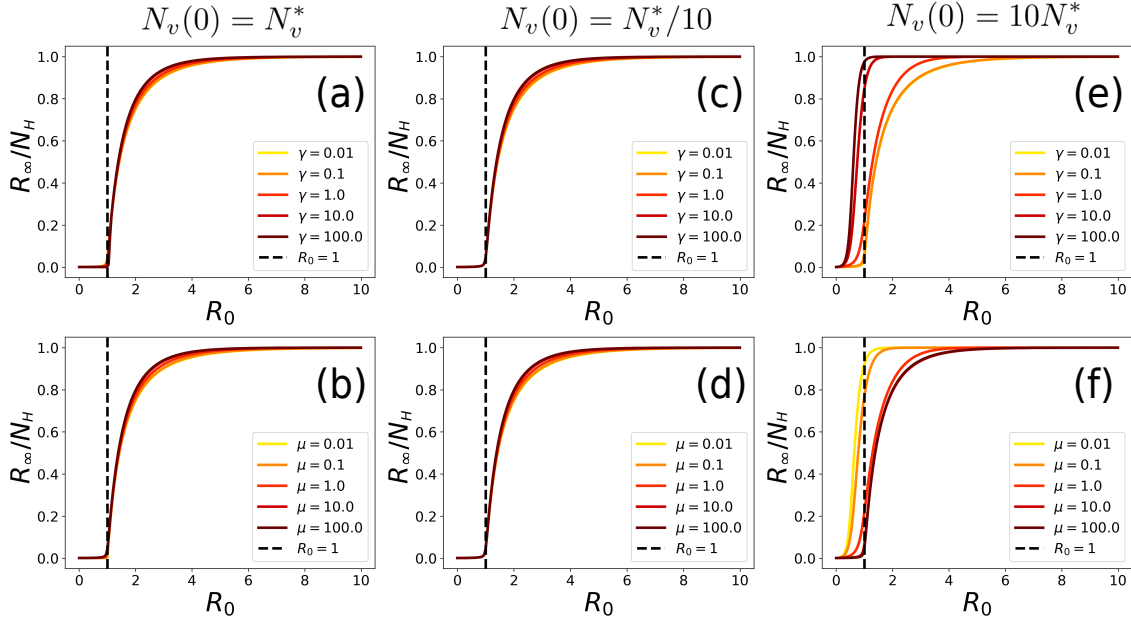


Figure 2: Numerical verification of the predictive power of the basic reproduction number relation Eq. (7), by plotting the final size of the epidemic, R_∞/N_H as function of R_0 . In panels (a),(b) the initial vector population is in the stationary value, in panels (c),(d) is below, $N_v^*/10$, and in panels (e),(f) above, $10N_v^*$. Panels (a),(c),(e) show realisations for different γ values with a fixed $\mu = 1$ baseline value. Panels (b),(d),(f) show realisations for different μ values with a fixed $\gamma = 1$ baseline value.

the initial disease free state of the model, given by $I_H(0) = I_v(0) = 0$, is a fixed point (equilibrium state) of the dynamical system Eq. (2) independently of the other initial conditions for the host and vector populations. This allows the definition of the basic reproduction number, R_0 , using standard methods such as linear stability analysis or the Next-Generation Matrix (NGM) method (Diekmann et al., 2010) (see Appendix A).

The situation is different when $\delta \neq \mu$, as then the total vector population will vary with time if the initial condition, $N_v(0)$, is not identical to the asymptotic value at large times, N_v^* , and thus an initial disease-free state is not an equilibrium (fixed point) of the model. However, in the literature it is customary to apply the standard techniques, i.e. NGM, to compute R_0 using the vector population in the asymptotic state, that is the post-pandemic disease-free equilibrium (Wei et al., 2008; Lashari & Zaman, 2011; Shah & Jyoti, 2013; Zhao et al., 2020; Esteva & Vargas, 1998). The use of these methods is supported by the fact that the asymptotic dynamics of the model converges to the dynamics of the subsystem where the vector population is stationary (Thieme, 1992; Castillo-Chavez & Thieme, 1995). In both cases the basic reproduction number is given by,

$$R_0 = \frac{\beta\alpha S_H(0)}{\mu\gamma} \frac{N_v^*}{N_H}. \quad (7)$$

As usual, R_0 accounts for the number of secondary infections produced by an infected individual in one generation and controls the threshold behaviour of the model: for $R_0 < 1$ the epidemic dies out and for $R_0 > 1$ an outbreak occurs. By one generation we refer to the typical time in which new infections can be produced, being the generation time in our model,

$$t_g = 1/\gamma + 1/\mu. \quad (8)$$

Here we show that this result can only be used in the more general case provided that some conditions are fulfilled, but not *always*. Let us first illustrate the different regimes in which Eq. (7) is predictive or not about the onset of the epidemic. In Fig. 2 the final size of the epidemic, R_∞/N_H , is plotted as a function of R_0 . Fig. 2(a)-(d) show that Eq. (7) does indeed regulate the onset of an epidemic when the initial vector population is in its stationary value or below it. This result is general and does not depend on the time-scales of the system, $1/\gamma$ and $1/\mu$, and so all curves

in these panels behave similarly. In contrast, Fig. 2(e)-(f) shows how the R_0 calculated according to Eq. (7) is not predictive of the onset of epidemic outbreak, this happening when the initial vector population is larger than the stationary value. Thus, for $R_0 < 1$ (computed using Eq. (7)) severe outbreaks appear, yielding mortalities even above 80% of the total population. However, one can observe that as μ is increased, or γ decreased, the predictive power of Eq. (7) is progressively recovered.

The observed behaviour and the regimes of validity of Eq. (7) can be explained readily. In essence, only if the vector population reaches its stationary value before infected hosts have produced new infections the onset of an epidemic can be characterised by Eq. (7), but not otherwise. Given these different behaviours, let us discuss separately the cases $f > 1$ and $f < 1$, with $N_v(0) = fN_v^*$, namely when the initial vector population is above and below its stationary value, this is, decaying and growing vector populations towards the asymptotic value.

Let us start with the case of decaying vector populations, $f > 1$. From Eq. (6), the time to approach the stationary value, t^* , fulfils

$$(1 + \epsilon) N_v^* = N_v^* \left[1 + (f + 1)e^{-\mu t^*} \right], \quad (9)$$

where $\epsilon \rightarrow 0$ is a small parameter controlling the amount by which the vector population differs from its asymptotic value at time t^* . Thus, the time to approach the stationary value, with precision ϵ , is given by

$$t^* = -\frac{1}{\mu} \ln \left(\frac{\epsilon}{f-1} \right) = \frac{1}{\mu} \left| \ln \frac{\epsilon}{f-1} \right|, \quad (10)$$

where the last equality assumes that the small parameter ϵ satisfies $\epsilon < (f-1)$, $f > 1$.

If the vector population reaches its stationary value before infected hosts have had time to generate new infections then R_0 as determined from Eq. (7) is a good prediction of the onset for an epidemic, what is equivalent to the condition that t^* is much smaller than the hosts infectious period, $t^* \ll 1/\gamma$,

$$\frac{1}{\gamma} \gg \frac{1}{\mu} \left| \ln \frac{\epsilon}{f-1} \right| \quad \text{or} \quad \frac{\mu}{\gamma} \gg \left| \ln \frac{\epsilon}{f-1} \right|. \quad (11)$$

Otherwise, Eq. (7) will not be predictive of the epidemic onset, and as shown in Fig. 2(e-f) one may have outbreaks with a substantial final size with $R_0 < 1$.

In the case of growing vector populations, $f < 1$, if $R_0 < 1$ an outbreak cannot occur at all, because R_0 is calculated with the asymptotic population, N_v^* , that is larger than the vector population at any finite time, $N_v(t) < N_v^* \forall t$, and so the threshold condition is never attained. In the $R_0 > 1$ case the behaviour will be richer, and it will depend on the initial condition, $N_v(0)$. One can define an instantaneous basic reproductive number,

$$R_0^{(i)}(t) = \frac{\beta\alpha}{\mu\gamma} \frac{S_H(0)}{N_H} N_v(t) = R_0 \frac{N_v(t)}{N_v^*}, \quad (12)$$

using $N_v(t)$ instead of N_v^* , with $R_0^{(i)}(t) < R_0 \forall t$ because the vector population grows. In particular, if $R_0^{(i)}(0) > 1$ there will be an outbreak occurring for short times, and the population of infected hosts will start growing. If instead, $R_0^{(i)}(0) < 1$, and as $R_0 > 1$ with R_0 being calculated with the asymptotic state, there must be an intermediate time, say t_D , for which $R_0^{(i)}(t_D) = 1$. Thus, from $t > t_D$ an outbreak will occur, not initially but after a finite time, that induces a delay in the outbreak, and the infected host population will start growing.

The difference between the original and the delayed dynamics stems from the waiting time to reach $R_0^{(i)} = 1$, t_D , plus the non-linear effect associated to a new initial condition for the epidemic outbreak at t_D . Thus, in the case that $R_0 > 1$ and $R_0^{(i)}(0) < 1$, from Eq. (12) and Eq. (6) we can analytically approximate the delay as the time needed to reach $R_0^{(i)}(t_D) = 1$,

$$1 + (f-1)e^{-\mu t_D} = \frac{1}{R_0}, \quad (13)$$

which yields the relation,

$$t_D = -\frac{1}{\mu} \ln \left[\frac{1 - R_0}{(f - 1) R_0} \right] , \quad (14)$$

where the argument of the logarithm is always positive because $R_0 > 1$ and $f < 1$. Eq. (14) is only valid if $f < 1/R_0$, for $R_0^{(i)}(0) = fR_0 < 1$, as if otherwise $R_0^{(i)} > 1$ the outbreak would already occur initially.

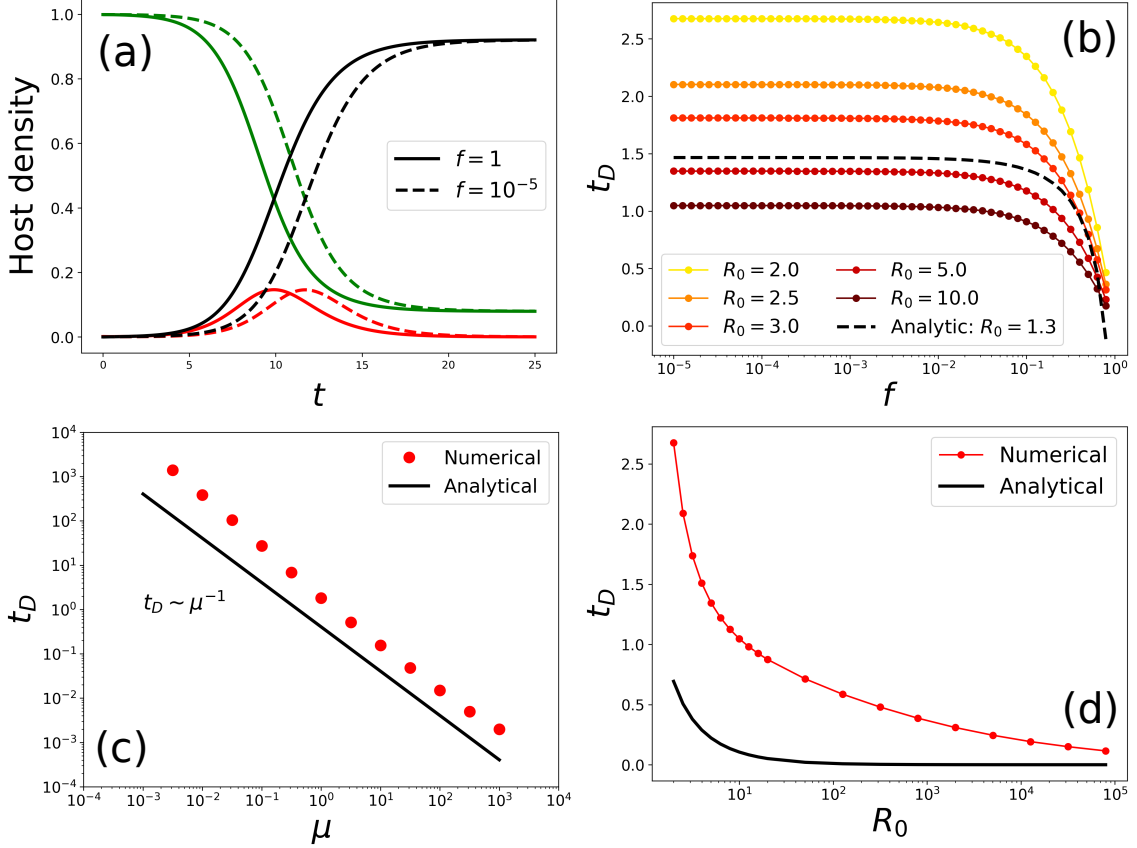


Figure 3: Numerical study of the delay induced by growing vector populations. (a) Comparison of hosts dynamics for a stationary vector population ($f = 1$) and a growing vector population ($f = 10^{-5}$). (b) Time delay as function of f for different values of the basic reproduction number R_0 . (c) Time delay as function of the vector natural death rate. (d) Time delay as function of the basic reproduction number, R_0 , with $f = 10^{-5}$.

From Eq. (14) one can see that when the initial vector population is far enough from its stationary value, $f \rightarrow 0$, the delay saturates to a constant value, instead of increasing. This is,

$$\lim_{f \rightarrow 0} t_D = -\frac{1}{\mu} \ln \left(\frac{R_0 - 1}{R_0} \right) = \frac{1}{\mu} \ln \left(\frac{R_0}{R_0 - 1} \right) . \quad (15)$$

In addition, for increasing values of the basic reproduction number, R_0 , the delay tends to vanish, and from Eq. (15). This is,

$$\lim_{R_0 \rightarrow \infty} t_D = \frac{1}{\mu} \ln(1) = 0 , \quad (16)$$

where the limit $f \rightarrow 0$ is taken simultaneously to guarantee that $R_0^{(i)}(0) = fR_0 < 1$. On the other hand the delay, t_D , scales with the vectors lifetime,

$$t_D \sim \frac{1}{\mu} = \tau_v . \quad (17)$$

Fig. 3(a) shows an example of the time delay caused in the hosts dynamics when the vector population grows from an initial condition far from the stationary value. In Fig. 3(b) we can

qualitatively observe that all the predicted properties of the delay are fulfilled, namely, the time delay saturates for low f values and decreases with increasing R_0 . Although the analytical expression (black dashed line) is clearly not exact due to nonlinear effects, Eq. (14) captures the basic trends of the time delay, t_D . This is clear from Fig. 3(c), that shows that the delay scales with $1/\mu$ and in Fig. 3(d) that shows that the delay tends to 0 in the limit $R_0 \rightarrow \infty$, in agreement with the prediction of Eq. (16).

3.2. The basic reproduction number for non-stationary vector populations

As shown in the previous section, traditional methods to compute the basic reproduction number fail in the case of epidemic models with decaying vector populations, $f > 1$, unless the time scale of vector population fulfils several conditions, as illustrated in Section 3.1. Here we introduce an effective, average definition of R_0 , useful to predict the epidemic onset for vector-borne diseases with decaying vector populations, i.e. the case where traditional methods fail. It is defined as the *average* number of infections produced by an infected individual in *one generation* Eq. (8),

$$\bar{R}_0 = \langle R_0^i(t) \rangle \Big|_0^{t_g} = R_0 \left[1 - \frac{1}{\tau} (f - 1) (e^{-\tau} - 1) \right] = R_0 \cdot \mathcal{F} \quad (18)$$

where $\tau = 1 + \mu/\gamma$ and \mathcal{F} is the expression in brackets accounting for the effect of the decaying vector population on the stationary R_0 (see Appendix B for the full derivation of Eq. (18)).

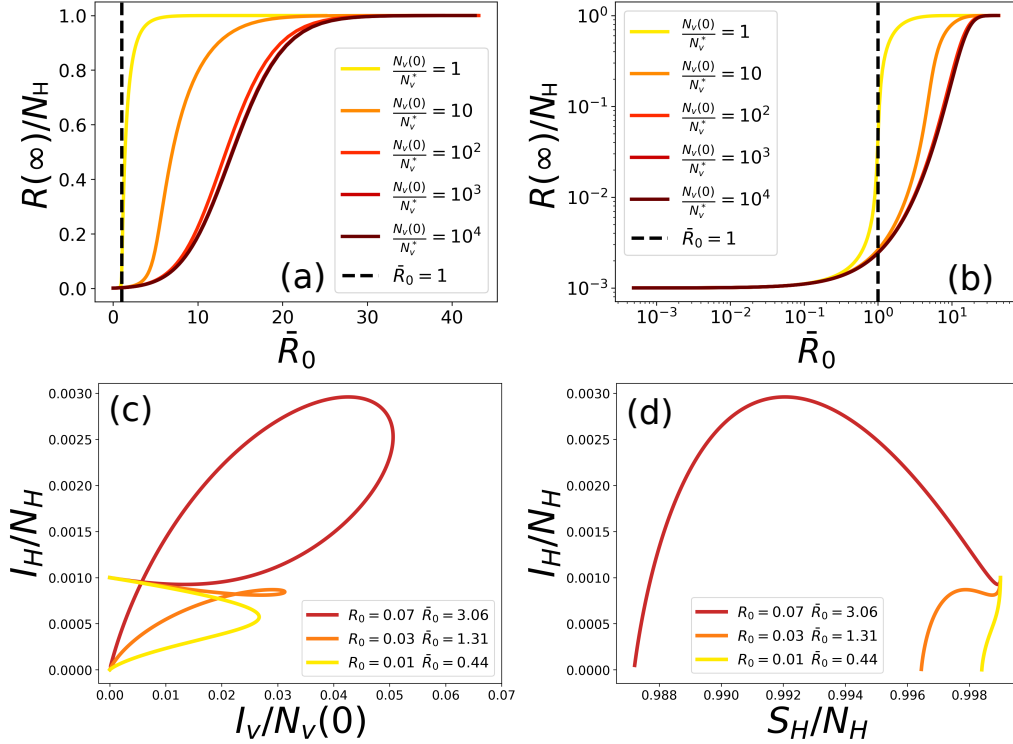


Figure 4: Numerical verification of the expression for the basic reproduction number for vector-borne diseases with decaying vector populations Eq. (18). Final size of the epidemic as a function of the basic reproduction number in panels: (a) linear scale; (b) logarithmic scale. Phase space trajectories in panels: (c) I_H/N_H vs $I_v/N_v(0)$ and (d) I_H/N_H vs S_H/N_H , where an initial condition $I_H(0)/N_H = 0.01$, $S_H(0)/N_H = 0.99$ and $I_v(0)/N_v(0) = 0$ has been used for the 3 cases. $\mu = \gamma$ has been used in all the simulations.

A first observation is that $\bar{R}_0 > R_0$ always. This stems from the fact that $\tau > 1$, so that $e^{-\tau} - 1 < 0$, and $f - 1 > 0$, which yields $\mathcal{F} > 1$. This discussion unravels why standard methods fail to predict the onset of an epidemic under decaying vector populations. Another important point is that if $\mu/\gamma \gg 1$, which implies $\tau \gg 1$, then $\bar{R}_0 \rightarrow R_0$ as,

$$\lim_{\tau \gg 1} \mathcal{F} = \lim_{\tau \gg 1} \left[1 - \frac{1}{\tau} (f - 1) (e^{-\tau} - 1) \right] = 1 + \frac{f - 1}{\tau}, \quad (19)$$

and if furthermore $\tau \sim \frac{\mu}{\gamma} \gg (f - 1)$ then $\mathcal{F} \rightarrow 1$ and $\overline{R_0} \rightarrow R_0$. This is in agreement with the discussion in [Section 3.1](#) showing that the R_0 computed from standard methods works if $\mu \gg \gamma$.

[Fig. 4\(a-b\)](#) contrasts numerically the validity of [Eq. \(18\)](#) to predict the final size of the epidemic as a function of the general basic reproduction number, $\overline{R_0}$, in linear and logarithmic scale, respectively. We observe that, independently of the initial condition of vectors, the outbreak occurs for $\overline{R_0} > 1$. However, we may notice that for large values of the initial condition of vectors the final size of the epidemic grows more slowly, so that larger values of $\overline{R_0}$ are needed to produce a proper outbreak. This can be explained by the fact that for $\overline{R_0}$ slightly above the threshold, $\overline{R_0} = 1$, and large values of $f = N_v(0)/N_v^*$, infections are produced only in the transient period of the dynamics, as $R_0 < 1$. This is, while the vector population is decaying to its stationary value, the vectors are able to produce new infections, but once the vector population reaches the stationary value, the epidemics stops. This transmission mechanism is radically different to that of vector-borne diseases with stationary vector populations in which the pre-pandemic disease-free state is an equilibrium of the system. The phase-space plots in [Fig. 4\(c-d\)](#) show that the time-averaged basic reproduction number $\overline{R_0}$ is able to accurately predict the conditions under which the infected host population will grow, in contrast with R_0 computed in the post-pandemic fixed point. In essence, for $\overline{R_0} > 1$ the infected host population, I_H , grows before reaching the absorbing state, $I_H = I_v = 0$, while for $\overline{R_0} < 1$ the infected host population is monotonically decreasing. We note that [Eq. \(18\)](#) is similar to the time-averaged basic reproduction number presented in ([Wesley & Allen, 2009](#)) for the periodic case, which is a first-order approximation to the *true* basic reproductive number ([Bacaër & Guernaoui, 2006](#)).

3.3. Fast-slow approximation

The original 5-D [Eq. \(2\)](#) model is certainly not amenable to mathematical analyses due to its high phase-space dimensionality and the fact that it depends on 4 parameters. Moreover, in a real-case application, if the parameters conforming the model are not known the model could suffer from parameter unidentifiability. However, some approximations can be performed to reduce the mathematical complexity of the model, as for instance a fast-slow (or adiabatic) approximation.

If the time-scale of the vector population evolution is faster than that of the infected hosts, what is expected to be a good approximation in many practical cases, the vector population will almost instantaneously adapt to its stationary value. Thus, if $1/\mu \ll 1/\gamma$, or equivalently if $\mu \gg \gamma$, we can rewrite the time derivative of the vector infected population as

$$\epsilon \dot{I}_v = \frac{\alpha}{\mu} S_v \frac{I_H}{N_H} - I_v, \quad (20)$$

with $\epsilon = 1/\mu$ being a small parameter. Then, \dot{I}_v can be neglected and the infected vector population can be obtained from the relationship,

$$I_v \approx \frac{\alpha}{\mu} \frac{S_v I_H}{N_H}. \quad (21)$$

Substituting [Eq. \(21\)](#) into the original system [Eq. \(2\)](#) and the identity $N_v(t) = S_v(t) + I_v(t)$ we obtain the following reduced system,

$$\begin{aligned} \dot{S}_H &= -\frac{\beta \alpha N_v(t)}{\mu N_H + \alpha I_H} \frac{S_H I_H}{N_H} \\ \dot{I}_H &= \frac{\beta \alpha N_v(t)}{\mu N_H + \alpha I_H} \frac{S_H I_H}{N_H} - \gamma I_H \\ \dot{R}_H &= \gamma I_H, \end{aligned} \quad (22)$$

which can be understood as a SIR model with time-dependent coefficients,

$$\begin{aligned} \dot{S}_H &= -\xi(t) \frac{S_H I_H}{N_H} \\ \dot{I}_H &= \xi(t) \frac{S_H I_H}{N_H} - \gamma I_H \\ \dot{R}_H &= \gamma I_H. \end{aligned} \quad (23)$$

A SIR model with time-dependent periodic coefficients was discussed in (Bacaër & Gomes, 2009).

Moreover, if $f \neq 1$ the above mentioned timescales relationship must fulfil $\frac{\mu}{\gamma} \gg \left| \ln \frac{\epsilon}{f-1} \right|$ (cf. Eq. (11)) and not only $\frac{\mu}{\gamma} \gg 1$. It is important to notice that the presence of horizontal transmission would simply rescale the coefficient $\xi(t)$, and the SIR reduction Eq. (23) would keep its validity.

In Fig. 5 we numerically verify the validity of the presented fast-slow approximation. As expected, we observe that the approximation breaks down for $\mu \sim \gamma$ (Fig. 5(a)), while as μ becomes larger than γ the approximation improves Fig. 5(b) and it becomes quantitative when $\mu \gg \gamma$, Fig. 5(c). Finally, we show in Fig. 5(d) a comparison between the dynamics of the hosts using both the original and the approximated model using the same parameters than in Fig. 5(c), where the results of both models are expected to converge.

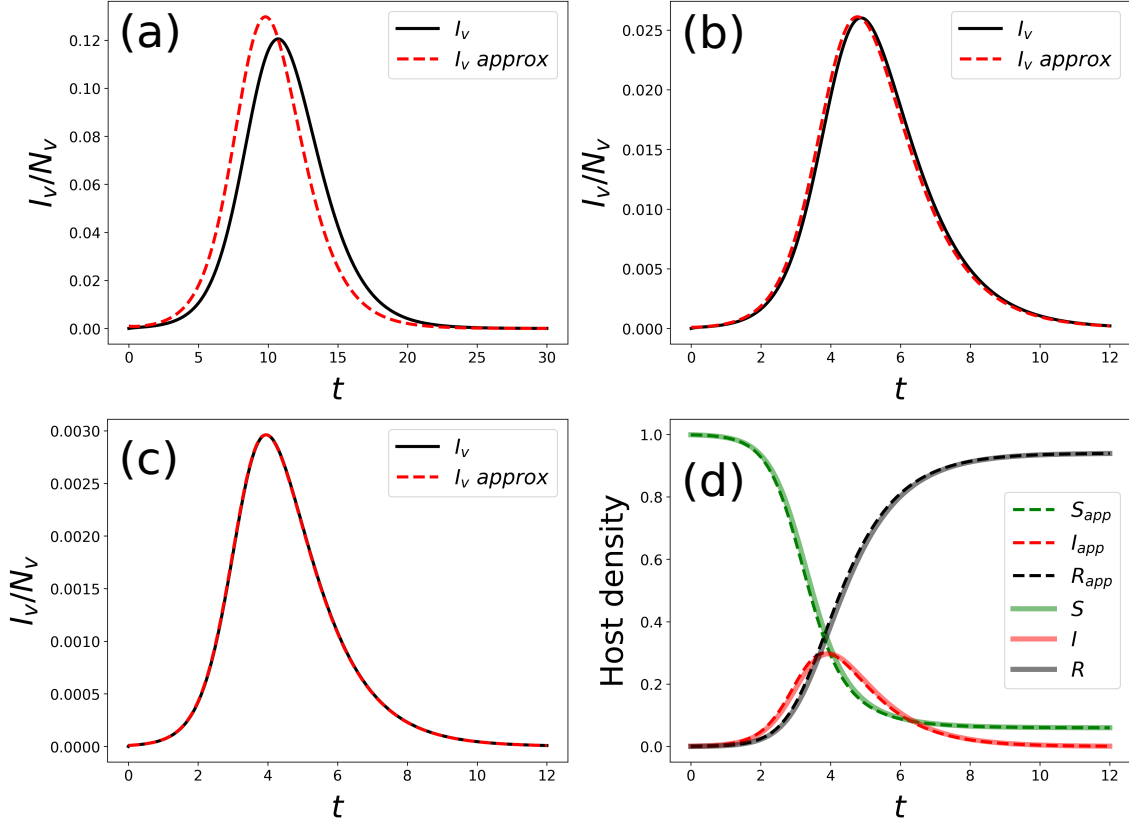


Figure 5: Numerical verification of the time-scale approximation (Eq. (21)) with $N_H = 100$, $\alpha = \gamma = 1$. β is chosen such that $R_0 = 3$. (a) $\mu = 1$, (b) $\mu = 10$, (c) $\mu = 100$. Panel (d) shows a comparison between the approximate and original models for the parameters used in (c), where the approximated models is expected to represent well the original one.

3.4. Reduction to a SIR model

The conditions for which the time-scale approximation is valid, $\mu \gg \gamma$, imply that the vector population will reach its stationary value almost instantaneously, so that $N_v(t) \approx N_v^*$. Thus, the system in Eq. (22) can be written approximately as the following SIR-like model,

$$\begin{aligned} \dot{S}_H &= -\beta' \frac{S_H I_H}{\lambda N_H + I_H} \\ \dot{I}_H &= \beta' \frac{S_H I_H}{\lambda N_H + I_H} - \gamma I_H \\ \dot{R}_H &= \gamma I_H, \end{aligned} \tag{24}$$

where $\beta' = \beta N_v^*/N_H$ and $\lambda = \mu/\alpha$.

Furthermore, if $\lambda N_H \gg I_H$ (which is indeed plausible in this limit) Eq. (24) the model can be written as a SIR model with constant coefficients,

$$\begin{aligned}\dot{S}_H &= -\beta_{eff} \frac{S_H I_H}{N_H} \\ \dot{I}_H &= \beta_{eff} \frac{S_H I_H}{N_H} - \gamma I_H \\ \dot{R}_H &= \gamma I_H ,\end{aligned}\tag{25}$$

where $\beta_{eff} = \frac{\beta'}{\lambda} = \frac{\beta \alpha N_v^*}{\mu N_H}$.

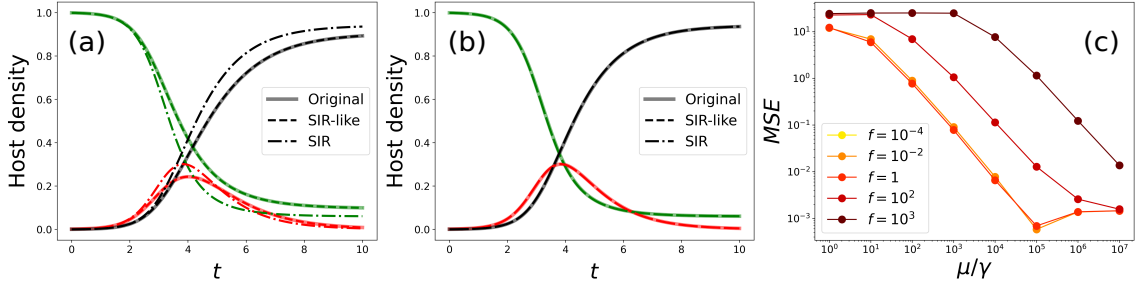


Figure 6: Comparison between the original model and the reductions, Eq. (24) (SIR-like) and Eq. (25) (SIR) with $N = 100$, $\mu/\gamma = 10^3$ and $f = 1$. β was chosen such that $R_0 = 3$. (a) $\lambda = 1$, (b) $\lambda = 10^{-3}$, (c) Mean Squared Error between the original model and the SIR approximations as function of the ratio μ/γ and f .

In Fig. 6 we show the validity of the reduced models Eq. (24) and Eq. (25). Fig. 6(a) shows that the SIR-like model (Eq. (24)) works when the time-scale approximation can be performed (as $\mu/\gamma \gg 1$) but the SIR model fails when the condition $\lambda N_H \gg I_H$ is not fulfilled. Conversely, in Fig. 6(b) we show that as $\lambda N_H \gg I_H$ is fulfilled, then the SIR model perfectly matches the original model. Finally, Fig. 6(c) shows the decrease in the mean squared error of the approximation as the condition Eq. (11) is fulfilled for different values of f .

4. Conclusions

In the present work we have analysed several features of a compartmental deterministic model for vector-borne diseases with 3 compartments for hosts and 2 for vectors, that does not consider neither horizontal nor vertical transmission. The focus is to study the behaviour of the model in the case that the vector population is not stationary. In this case, the pre-pandemic disease-free state is not a fixed point (equilibrium state) of the dynamical system, and, in principle, the methods that are customarily used to determine the basic reproduction number, R_0 do not work. This is so because these methods determine the onset of an outbreak by performing a linear stability analysis of the disease-free state, assuming that it is a fixed point of the model. A common assumption made in the literature is to determine R_0 from the asymptotic state for the vectors (if it is not an extinction state).

We have analysed several initial conditions of the vector population, characterising different regimes. In the case that the initial condition for the number of vectors is below the asymptotic state, implying that the vector population overall grows, then R_0 as determined from the asymptotic state correctly predicts the existence (or not) of an epidemic outbreak, but with a temporal delay in its appearance. This result contrasts with the situation in which the initial state is above the asymptotic state, with an overall decrease in the vector population. In this case R_0 determined from the asymptotic state may fail badly, predicting no outbreak while a large fraction of the population might get infected. We present a simple, albeit useful, generalisation of R_0 that is able to give a reasonable prediction of the epidemic threshold for decaying populations, including the case in which vectors become extinct, a case in which the asymptotic estimation to determine R_0 cannot be applied.

Compartmental models of vector-borne diseases usually have many compartments and parameters, which can lead to a problem of parameter unidentifiability. The model analysed here is not an exception, and when applied to real-world cases many different combinations of the parameters could be able to reproduce the available data. Thus, in order to facilitate the application of the model to experimental data, we have studied a useful fast-slow (or adiabatic) approximation that allows to reduce the model if the parameters fulfil certain conditions. In particular, our study shows that under quite realistic assumptions (the typical timescale of hosts infection and death is much slower than vector timescales) it is possible to obtain a reduced SIR model. We recall that this reduction implies that, under these assumptions, the process by which hosts (that could be immobile) get infected through the action of vectors is equivalent to a direct interaction among hosts.

The deterministic compartmental model analysed here, with some modifications, is a clear candidate to study many vector-borne diseases, in particular phytopathologies. Furthermore, in case of parameter unidentifiability the model reductions performed in this work could be useful to solve this issue. In any case, this description is still idealised, as compartmental models imply a well-mixed assumption in which space is not explicitly described. This kind of representations are not always applicable to real-world scenarios although are useful as a first approximation. Thus, future research should focus on the integration of space and vector mobility in the model to account for more realistic situations.

Acknowledgments

AGR and MAM acknowledge financial support from Grant RTI2018-095441-B-C22 (SuMaEco) funded by MCIN/AEI/10.13039/501100011033 and by “ERDF A way of making Europe” and from the María de Maeztu Program for Units of Excellence in R&D (No. MDM-2017-0711).

Appendix A. Calculation of R_0 from standard methods

The standard methods of calculation of R_0 are based in the linear stability analysis of the disease-free equilibrium, either directly, through the linear analysis of the fixed point, that yields the stability condition from which R_0 can be obtained, or using the Next Generation Method (NGM) (Diekmann et al., 2010) that provides directly R_0 by solving a suitable linear problem. Customarily these methods are applied to a pre-pandemic disease-free equilibrium, but as there is no such state in the case of non-stationary populations, here a similar approach is applied to a post-pandemic or asymptotic disease-free equilibrium.

Linear stability analysis

In order to perform the linear stability analysis of the fixed point ($I_H = I_v = 0$) we first need to compute the Jacobian matrix, J ,

$$J = \begin{pmatrix} -\beta \frac{I_v}{N_H} & 0 & 0 & -\beta \frac{S_H}{N_H} \\ \beta \frac{I_v}{N_H} & -\gamma & 0 & \beta \frac{S_H}{N_H} \\ 0 & -\alpha \frac{S_v}{N_H} & -\alpha \frac{I_H}{N_H} - \mu & 0 \\ 0 & \alpha \frac{S_v}{N_H} & \alpha \frac{I_H}{N_H} & -\mu \end{pmatrix} \quad (\text{A.1})$$

Then, we evaluate the Jacobian at the fixed point (or disease free equilibrium, DFE), yielding

$$J|_{DFE} = \begin{pmatrix} 0 & 0 & 0 & -\beta \\ 0 & -\gamma & 0 & \beta \\ 0 & -\alpha \frac{C}{N_H} \frac{\delta}{\mu} & -\mu & 0 \\ 0 & \alpha \frac{C}{N_H} \frac{\delta}{\mu} & 0 & -\mu \end{pmatrix} \quad (\text{A.2})$$

where $S_H = N_H$ has been considered.

Finally, we obtain the eigenvalues of this matrix as

$$\begin{aligned} \det(J|_{DFE} - \lambda \mathbb{I}) &= -\lambda \left[-(\mu + \lambda)^2(\gamma + \lambda) + (\mu + \lambda)\beta\alpha \frac{C}{N_H} \frac{\delta}{\mu} \right] = 0 \Rightarrow \\ \lambda_0 &= 0 \\ \lambda_\mu &= -\mu \\ \lambda_\pm &= -\frac{(\gamma + \mu)}{2} \pm \frac{1}{2} \sqrt{(\gamma - \mu)^2 + 4\beta\alpha \frac{C}{N_H} \frac{\delta}{\mu}} \end{aligned} \quad (\text{A.3})$$

It is straightforward to see that all eigenvalues are real and the stability of the disease-free equilibrium is determined by the sign of the eigenvalues. $\lambda_\mu = -\mu < 0$ as μ is defined positive, so in order to discuss the stability of this fixed point, we need to study the λ_\pm eigenvalues. λ_- is always negative, but λ_+ changes sign depending on the values of the parameters. The threshold condition $\lambda_+ = 0$ leads to:

$$\lambda_+ = 0 \Rightarrow \frac{\beta\alpha}{\gamma\mu} \frac{C}{N_H} \frac{\delta}{\mu} = 1 \quad (\text{A.4})$$

So, for $\frac{\beta\alpha}{\gamma\mu} \frac{C}{N_H} \frac{\delta}{\mu} < 1 \Rightarrow \lambda_+ < 0$ the fixed point is stable and for $\frac{\beta\alpha}{\gamma\mu} \frac{C}{N_H} \frac{\delta}{\mu} > 1 \Rightarrow \lambda_+ > 0$ a perturbation will grow in the direction of the eigenvector associated to λ_+ . Thus, this threshold defines the basic reproduction number,

$$R_0 = \frac{\beta\alpha}{\gamma\mu} \frac{C}{N_H} \frac{\delta}{\mu} \quad (\text{A.5})$$

If instead of $S_H = N_H$ one considers any initial condition of hosts, $S_H(0)$, the basic reproduction number is given by,

$$R_0 = \frac{\beta\alpha}{\gamma\mu} \frac{C}{N_H} \frac{\delta}{\mu} \frac{S_H(0)}{N_H} \quad (\text{A.6})$$

Next Generation Matrix method

The previous result can also be obtained by means of the NGM method, which is explained in detail in (Diekmann et al., 2010). Basically the method is based in decomposing the Jacobian in the form $\mathbf{J} = \mathbf{T} + \mathbf{\Sigma}$, where \mathbf{T} is the *transmission part*, that describes the production of new infections, and $\mathbf{\Sigma}$ the *transition part*, that describes changes of state (including death). Then, it can be proved (Diekmann et al., 2010) that the *basic reproduction number* R_0 is given by the spectral radius (i.e. the largest eigenvalue) of the (next generation) matrix $\mathbf{K} = -\mathbf{T}\mathbf{\Sigma}^{-1}$.

$$\mathbf{K} = -\mathbf{T}\mathbf{\Sigma}^{-1} = \begin{pmatrix} \frac{\beta\alpha}{\gamma\mu} \frac{C}{N_H} \frac{\delta}{\mu} & \frac{\beta}{\mu} \\ 0 & 0 \end{pmatrix} \quad (\text{A.7})$$

with,

$$\mathbf{T} = \begin{pmatrix} 0 & \beta \frac{N_H}{N_H} \\ 0 & 0 \end{pmatrix} \quad \mathbf{\Sigma} = \begin{pmatrix} -\gamma & 0 \\ \alpha \frac{C}{N_H} \frac{\delta}{\mu} & -\mu \end{pmatrix} \Rightarrow -\mathbf{\Sigma}^{-1} = \begin{pmatrix} \frac{1}{\gamma} & 0 \\ \frac{\alpha}{\gamma\mu} \frac{C}{N_H} \frac{\delta}{\mu} & \frac{1}{\mu} \end{pmatrix} \quad (\text{A.8})$$

The basic reproduction number is the spectral radius of this matrix so:

$$\begin{aligned} \det(\mathbf{K} - \sigma \mathbb{I}) &= 0 \Rightarrow \begin{vmatrix} \frac{\beta\alpha}{\gamma\mu} \frac{C}{N_H} \frac{\delta}{\mu} - \sigma & \frac{\beta}{\mu} \\ 0 & -\sigma \end{vmatrix} = (-\sigma) \left(\frac{\beta\alpha}{\gamma\mu} \frac{C}{N_H} \frac{\delta}{\mu} - \sigma \right) = 0 \Rightarrow \\ \sigma &= \frac{\beta\alpha}{\gamma\mu} \frac{C}{N_H} \frac{\delta}{\mu}; \quad \sigma = 0 \end{aligned} \quad (\text{A.9})$$

Therefore, the basic reproduction number is

$$R_0 = \frac{\beta\alpha}{\gamma\mu} \frac{C}{N_H} \frac{\delta}{\mu} \quad (\text{A.10})$$

If instead of $S_H = N_H$ one considers any initial condition of hosts, $S_H(0)$, the basic reproduction number is given by,

$$R_0 = \frac{\beta\alpha}{\gamma\mu} \frac{C}{N_H} \frac{\delta}{\mu} \frac{S_H(0)}{N_H} \quad (\text{A.11})$$

Appendix B. Calculation of R_0 for non-stationary vector populations

A simple way of extending the definition of R_0 in the case of non-stationary vector populations consists of averaging the number of secondary infections produced by an infected individual along one generation, that is equivalent to averaging the instantaneous definition of R_0 , namely R_0^i , over one generation,

$$\overline{R_0} = \langle R_0^i(t) \rangle \Big|_0^{t_g} = \frac{R_0}{N_v^*} \langle N_v(t) \rangle \Big|_0^{t_g} = \frac{R_0}{N_v^*} \frac{1}{t_g} \int_0^{t_g} N_v(t) dt , \quad (\text{B.1})$$

where the integral in Eq. (B.1) is solved as

$$\int_0^{t_g} N_v(t) dt = \left[N_v^* t - \frac{1}{\mu} (N_v(0) - N_v^*) e^{-\mu t} \right]_0^{t_g} = N_v^* t_g - \frac{1}{\mu} (N_v(0) - N_v^*) [e^{-\mu t_g} - 1] . \quad (\text{B.2})$$

Thus, the basic reproduction number for non-stationary vector populations is given by

$$\overline{R_0} = \frac{R_0}{N_v^*} \left\{ N_v^* - \frac{1}{\mu t_g} [N_v(0) - N_v^*] [e^{-\mu t_g} - 1] \right\} , \quad (\text{B.3})$$

where the generation time, t_g , is Eq. (8). Eq. (B.3) can be rewritten as,

$$\overline{R_0} = \langle R_0^i(t) \rangle \Big|_0^{t_g} = R_0 \left[1 - \frac{1}{\tau} (f - 1) (e^{-\tau} - 1) \right] = R_0 \cdot \mathcal{F} , \quad (\text{B.4})$$

where $\tau = 1 + \mu/\gamma$ and \mathcal{F} is the expression in brackets, which accounts for the effect of the decaying vector population on the stationary R_0 .

In our approach, a generation is defined as the time elapsed in the following sequence of processes: 1) A host individual becomes infected; 2) The infected host passes the disease to a susceptible vector; 3) The infected vector dies. Basically, the time elapsed from the first to the last process is the time in which new infections can be produced, i.e. t_g Eq. (8).

References

- Anderson, R. M. (1991). Discussion: The Kermack-McKendrick epidemic threshold theorem. *Bulletin of Mathematical Biology*, 53, 3–32. doi:[10.1016/S0092-8240\(05\)80039-4](https://doi.org/10.1016/S0092-8240(05)80039-4).
- Athni, T. et al. (2020). How vector-borne disease shaped the course of human history. doi:[10.22541/au.159135318.82566392](https://doi.org/10.22541/au.159135318.82566392).
- Bacaër, N. (2007). Approximation of the basic reproduction number r_0 for vector-borne diseases with a periodic vector population. *Bulletin of Mathematical Biology*, 69, 1067–1091. doi:[10.1007/s11538-006-9166-9](https://doi.org/10.1007/s11538-006-9166-9).
- Bacaër, N., & Gomes, M. G. M. (2009). On the final size of epidemics with seasonality. *Bulletin of Mathematical Biology*, 71, 1954. doi:[10.1007/s11538-009-9433-7](https://doi.org/10.1007/s11538-009-9433-7).
- Bacaër, N., & Guernaoui, S. (2006). The epidemic threshold of vector-borne diseases with seasonality. *Journal of Mathematical Biology*, 53, 421–436. doi:[10.1007/s00285-006-0015-0](https://doi.org/10.1007/s00285-006-0015-0).
- Bragard, C., Caciagli, P., Lemaire, O., Lopez-Moya, J., MacFarlane, S., Peters, D., Susi, P., & Torrance, L. (2013). Status and prospects of plant virus control through interference with vector transmission. *Annual Review of Phytopathology*, 51, 177–201. doi:[10.1146/annurev-phyto-082712-102346](https://doi.org/10.1146/annurev-phyto-082712-102346).
- Brauer, F. (2008). Compartmental models in epidemiology. In F. Brauer, P. van den Driessche, & J. Wu (Eds.), *Mathematical Epidemiology* (pp. 19–79). Berlin, Heidelberg: Springer Berlin Heidelberg. doi:[10.1007/978-3-540-78911-6_2](https://doi.org/10.1007/978-3-540-78911-6_2).
- Brauer, F., Castillo-Chavez, C., Mubayi, A., & Towers, S. (2016). Some models for epidemics of vector-transmitted diseases. *Infectious Disease Modelling*, 1, 79–87. doi:[10.1016/j.idm.2016.08.001](https://doi.org/10.1016/j.idm.2016.08.001).
- Castillo-Chavez, C., & Thieme, H. R. (1995). Asymptotically autonomous epidemic models. In D. Arino, O. Axelrod, M. Kimmel, & M. Langlais (Eds.), *Mathematical Population Dynamics: Analysis of Heterogeneity, Vol. I, Theory of Epidemics* (pp. 33–50). Wuerz publishing (Winnipeg). URL: <https://ecommons.cornell.edu/bitstream/handle/1813/31834/BU-1248-M.pdf>.
- Chowell, G. (2017). Fitting dynamic models to epidemic outbreaks with quantified uncertainty: A primer for parameter uncertainty, identifiability, and forecasts. *Infectious Disease Modelling*, 2, 379–398. doi:[10.1016/j.idm.2017.08.001](https://doi.org/10.1016/j.idm.2017.08.001).
- Diekmann, O., & Heesterbeek, J. A. P. (2000). *Mathematical Epidemiology of Infectious Diseases. Model Building, Analysis and Interpretation*. Chichester (UK): John Wiley and Sons.
- Diekmann, O., Heesterbeek, J. A. P., & Roberts, M. G. (2010). The construction of next-generation matrices for compartmental epidemic models. *Journal of The Royal Society Interface*, 7, 873–885. doi:[10.1098/rsif.2009.0386](https://doi.org/10.1098/rsif.2009.0386).
- Esteva, L., & Vargas, C. (1998). Analysis of a dengue disease transmission model. *Mathematical Biosciences*, 150, 131–151. doi:[10.1016/S0025-5564\(98\)10003-2](https://doi.org/10.1016/S0025-5564(98)10003-2).
- Garms, R., Walsh, J., & Davies, J. (1979). Studies on the reinvasion of the onchocerciasis control programme in the volta river basin by simulum damnosum si with emphasis on the south-western areas. *Tropenmedizin und Parasitologie*, 30, 345–362.
- Giménez-Romero, A., Grau, A., Hendriks, I. E., & Matias, M. A. (2021). Modelling parasite-produced marine diseases: The case of the mass mortality event of pinna nobilis. *Ecological Modelling*, 459, 109705. doi:[10.1016/j.ecolmodel.2021.109705](https://doi.org/10.1016/j.ecolmodel.2021.109705).
- Huang, W., Reyes-Caldas, P., Mann, M., Seifbarghi, S., Kahn, A., Almeida, R. P., Béven, L., Heck, M., Hogenhout, S. A., & Coaker, G. (2020). Bacterial vector-borne plant diseases: Unanswered questions and future directions. *Molecular Plant*, 13, 1379–1393. doi:[10.1016/j.molp.2020.08.010](https://doi.org/10.1016/j.molp.2020.08.010).

- Kamgang, J. C., & Sallet, G. (2008). Computation of threshold conditions for epidemiological models and global stability of the disease-free equilibrium (dfe). *Mathematical Biosciences*, 213, 1–12. doi:[10.1016/j.mbs.2008.02.005](https://doi.org/10.1016/j.mbs.2008.02.005).
- Kao, Y.-H., & Eisenberg, M. C. (2018). Practical unidentifiability of a simple vector-borne disease model: Implications for parameter estimation and intervention assessment. *Epidemics*, 25, 89–100. doi:[10.1016/j.epidem.2018.05.010](https://doi.org/10.1016/j.epidem.2018.05.010).
- Kermack, W. O., & McKendrick, A. G. (1927). A contribution to the mathematical theory of epidemics. *Proceedings of the Royal Society of London. Series A*, 115, 700–721. doi:[10.1098/rspa.1927.0118](https://doi.org/10.1098/rspa.1927.0118).
- Lashari, A. A., & Zaman, G. (2011). Global dynamics of vector-borne diseases with horizontal transmission in host population. *Computers & Mathematics with Applications*, 61, 745–754. doi:[10.1016/j.camwa.2010.12.018](https://doi.org/10.1016/j.camwa.2010.12.018).
- Laukó, I. G. (2006). Stability of disease free sets in epidemic models. *Mathematical and Computer Modelling*, 43, 1357–1366. doi:[10.1016/j.mcm.2005.06.011](https://doi.org/10.1016/j.mcm.2005.06.011).
- Macdonald, G. (1957). *The epidemiology and control of malaria*. Oxford (UK): Oxford University Press.
- Martcheva, M. (2015). *An Introduction to Mathematical Epidemiology*. New York: Springer. doi:[10.1007/978-1-4899-7612-3](https://doi.org/10.1007/978-1-4899-7612-3).
- Rocklöv, J., & Dubrow, R. (2020). Climate change: an enduring challenge for vector-borne disease prevention and control. *Nature Immunology*, 21, 479–483. doi:[10.1038/s41590-020-0648-y](https://doi.org/10.1038/s41590-020-0648-y).
- Roosa, K., & Chowell, G. (2019). Assessing parameter identifiability in compartmental dynamic models using a computational approach: application to infectious disease transmission models. *Theoretical Biology and Medical Modelling*, 16, 1. doi:[10.1186/s12976-018-0097-6](https://doi.org/10.1186/s12976-018-0097-6).
- Rybicki, E. P. (2015). A top ten list for economically important plant viruses. *Archives of Virology*, 160, 17–20. doi:[10.1007/s00705-014-2295-9](https://doi.org/10.1007/s00705-014-2295-9).
- Schneider, K., van der Werf, W., Cendoya, M., Mourits, M., Navas-Cortés, J. A., Vicent, A., & Oude Lansink, A. (2020). Impact of xylella fastidiosa subspecies pauca in european olives. *Proceedings of the National Academy of Sciences*, 117, 9250–9259. doi:[10.1073/pnas.1912206117](https://doi.org/10.1073/pnas.1912206117).
- Schumacher, S. K., & Campbell, J. I. (2018). Chapter 56 - travel medicine. In R. P. Olympia, R. M. O'Neill, & M. L. Silvis (Eds.), *Urgent Care Medicine Secrets* (pp. 352–357). Elsevier. doi:[10.1016/B978-0-323-46215-0.00056-2](https://doi.org/10.1016/B978-0-323-46215-0.00056-2).
- Shah, N., & Jyoti, G. (2013). SEIR model and simulation for vector borne diseases. *Applied Mathematics*, 4, 13 – 17. doi:[10.4236/am.2013.48A003](https://doi.org/10.4236/am.2013.48A003).
- Thieme, H. R. (1992). Convergence results and a Poincaré-Bendixson trichotomy for asymptotically autonomous differential equations. *Journal of Mathematical Biology*, 30, 755–763. doi:[10.1007/BF00173267](https://doi.org/10.1007/BF00173267).
- Tumber, K., Alston, J., Fuller, K. et al. (2014). Pierce’s disease costs California \$104 million per year. *California Agriculture*, 68, 20–29.
- van den Driessche, P. (2017). Reproduction numbers of infectious disease models. *Infectious Disease Modelling*, 2, 288–303. doi:[10.1016/j.idm.2017.06.002](https://doi.org/10.1016/j.idm.2017.06.002).
- Wei, H.-M., Li, X.-Z., & Martcheva, M. (2008). An epidemic model of a vector-borne disease with direct transmission and time delay. *Journal of Mathematical Analysis and Applications*, 342, 895–908. doi:[10.1016/j.jmaa.2007.12.058](https://doi.org/10.1016/j.jmaa.2007.12.058).
- Wesley, C. L., & Allen, L. J. (2009). The basic reproduction number in epidemic models with periodic demographics. *Journal of Biological Dynamics*, 3, 116–129. doi:[10.1080/17513750802304893](https://doi.org/10.1080/17513750802304893). PMID: 22880824.

WHO (2018). Fact sheets of vector-borne diseases. URL: https://www.hiobs.org/lib/file/manager/Vector-Borne_Disease_General_Fact_Sheet.pdf.

Zhao, S., Musa, S. S., Hebert, J. T., Cao, P., Ran, J., Meng, J., He, D., & Qin, J. (2020). Modelling the effective reproduction number of vector-borne diseases: the yellow fever outbreak in Luanda, Angola 2015-2016 as an example. *PeerJ*, 8, e8601–e8601. doi:[10.7717/peerj.8601](https://doi.org/10.7717/peerj.8601).